

Supporting Information for
Eugenol-Derived Molecular Glass: A Promising Biobased Material
in the Design of Self-Healing Polymeric Materials

Cong Li^{a}, Yizhou Chen^b, Xiaoxia Cai^c, Guihua Yang^a, Xiuzhi Susan Sun^{b*}*

^a *State Key Laboratory of Biobased Material and Green Papermaking, Qilu University of Technology (Shandong Academy of Sciences), No.3501, Daxue Road, Changqing District, Jinan, 250353 , PR China*

^b *Bio-Materials and Technology Lab, Department of Grain Science and Industry, Kansas State University, 1980 Kimball Ave, BIVAP Innovation Center, Manhattan, Kansas 66506 , USA*

^c *Key Laboratory of Processing and Testing Technology of Glass Functional Ceramics of Shandong Province, School of Materials Science and Engineering, Qilu University of Technology (Shandong Academy of Sciences), No.3501, Daxue Road, Changqing District, Jinan, 250353 , PR China*

** Co-corresponding Authors: Cong Li, E-mail: congli2016@163.com; Xiuzhi Susan Sun, E-mail: xss@ksu.edu, Phone: 785-532-4077, fax: 785-532-7193*

The supporting information included 17 pages, 12 figures and 2 tables.

^{*}Corresponding authors, Cong Li, E-mail address: congli2016@163.com ; Xiuzhi Susan Sun, E-mail address: xss@ksu.edu

Contents

1. Figure S1. Typical stress-strain curves of p-ESO, molecular glass ET-eugenol and its blends with p-ESO at variant fractions.	Page S3
2. Figure S2. ¹ H-NMR spectra of ep-Eugenol and ep-eugenol-12h.	Pages S4-S5
3. Figure S3. ¹ H-NMR spectra of ep-Eugenol with thermochemical conversion going on.	Pages S5-S6
4. Figure S4. Gas chromatography (GC) traces of Eugenol, ep-Eugenol and ep-Eugenol-12h.	Page S7
5. Figure S5. Moieties identified in the eugenol system.	Pages S8-S9
6. Figure S6. Heating and cooling DSC loop tests for ET-eugenol molecular glass.	Page S10
7. Figure S7. SEM image of ET-eugenol/p-ESO (mass ratio of 1:2)	Page S11
8. Figure S8. DSC thermograms for p-ESO, ET-eugenol and ET-eugenol/p-ESO (mass ratio of 1:2)	Page S12
9. Figure S9. Swelling rate of p-ESO and insoluble content of ET-eugenol/p-ESO (mass ratio of 1:2)	Page S13
10. Figure S10. Ultraviolet-visible absorption spectra and Infrared image	Page S14
11. Figure S11. Comparison of shape stabilities of ET-eugenol and ET-eugenol/p-ESO.	Page S15
12. Figure S12. Stress relaxations and Creep test of ET-eugenol/p-ESO (mass ratio of 1:2)	Page S16-S17

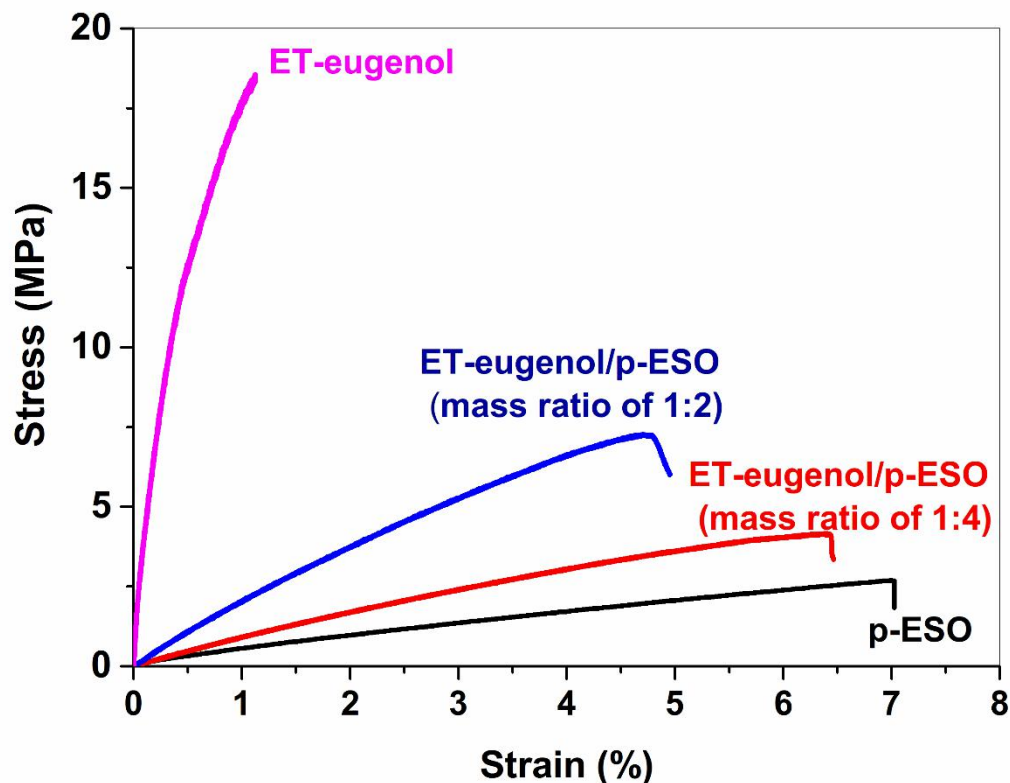
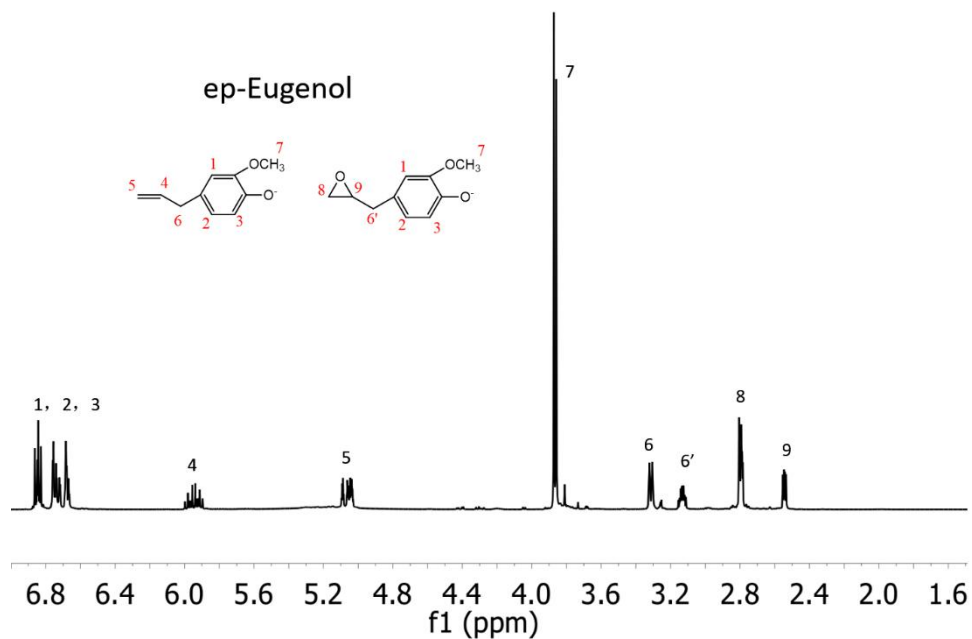


Figure S1. Typical stress-strain curves of p-ESO, molecular glass ET-eugenol and its blends with p-ESO at variant fractions.

Molecular glass ET-eugenol is quite brittle, as evidenced by the 1% breaking strain. Compared to the neat p-ESO, the incorporation of the ET-eugenol into p-ESO matrix led to an increase in tensile stress and a decrease in breaking strain. As expected, ET-eugenol/p-ESO (mass ratio of 1:2) shows a higher tensile stress and lower breaking strain in comparison with ET-eugenol/p-ESO (mass ratio of 1:4) due to the higher content of ET-eugenol.

1)



2)

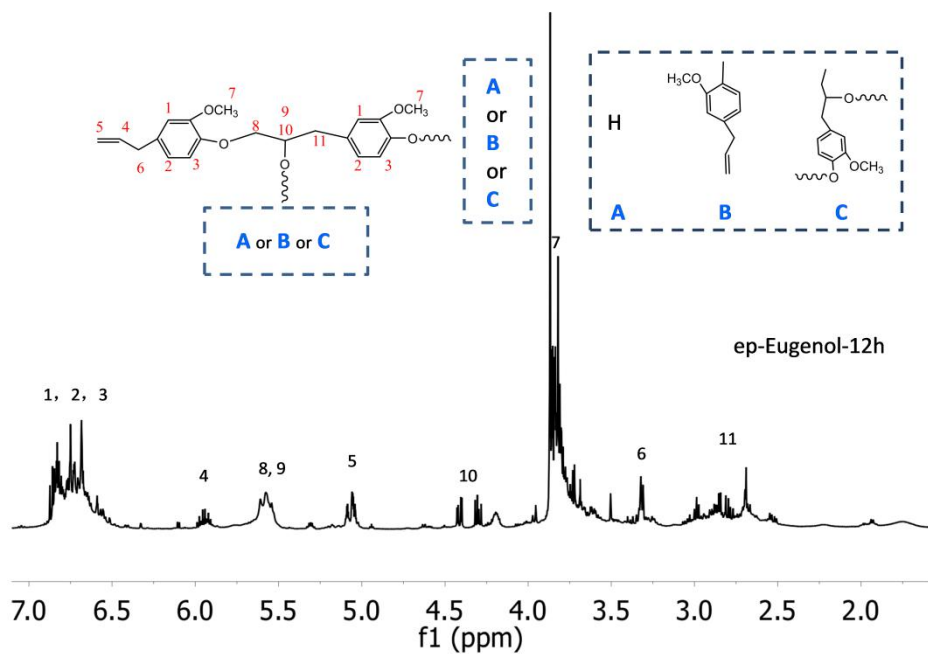


Figure S2. (1)¹H-NMR spectra of ep-Eugenol and (2) ep-eugenol-12h (typical chemical structures are shown). Here, ep-Eugenol is the derivate of eugenol after undergoing an epoxidation process at room temperature for 12 h; ep-Eugenol-12h is the derivate of ep-Eugenol after undergoing a thermochemical conversion at 170 °C for 12h.

Supporting Information

Chemical shift assignments of ep-Eugenol and ep-Eugenol-12h are listed above. Compared to ep-Eugenol, ep-Eugenol-12h demonstrated more complex signal peaks after the thermochemical conversion, and the typical motif is displayed in Figure S2-(2) to illustrate the corresponding chemical structures.

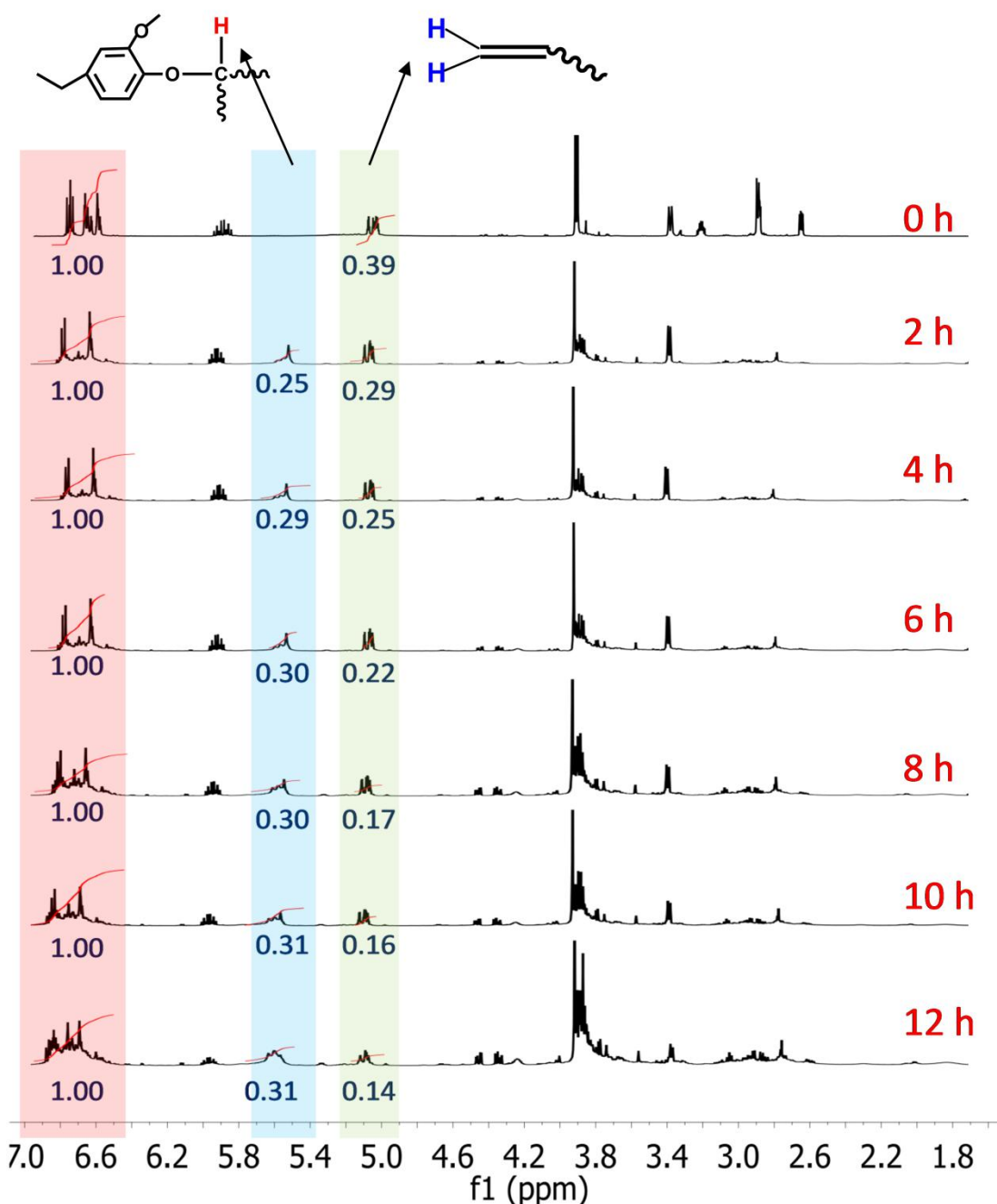


Figure S3. $^1\text{H-NMR}$ spectra of ep-Eugenol after undergoing varying time of thermochemical conversion at $170\text{ }^\circ\text{C}$.

Supporting Information

As Figure S3 shows, peaks centered at 5.6 ppm appeared after ep-Eugenol undergoing a thermochemical conversion, which are attributed to the protons connected by the *PhOCH~* moiety. The conversion trend of methoxyphenol moiety in the thermochemical conversion process can be estimated by the equation below, where I_1 is the signal integral of H atoms at 5.7-5.4 ppm, and I_2 is the signal integral of H atoms at 7.0-6.5 ppm, i.e., the H atoms on the phenyl ring. Here, the signal integral of H atoms on the phenyl ring are normalized as 1 and used as the internal standard considering no chemical reactions occur on these sites.

$$\text{Conversion}_{\text{PhOCH~ moiety}}(\%) = 100 \times I_1 / I_2$$

Peaks centered at 5.1 ppm are attributed to the protons on the terminal alkene group, and its conversion trend in the thermochemical conversion process is estimated by the equation below, where I_3 is the signal integral of H atoms at 5.2-5.0 ppm, and 0.39 is its corresponding signal integral at thermochemical conversion time of 0 h.

$$\text{Conversion}_{\text{terminal alkene}}(\%) = 100 \times I_3 / 0.39$$

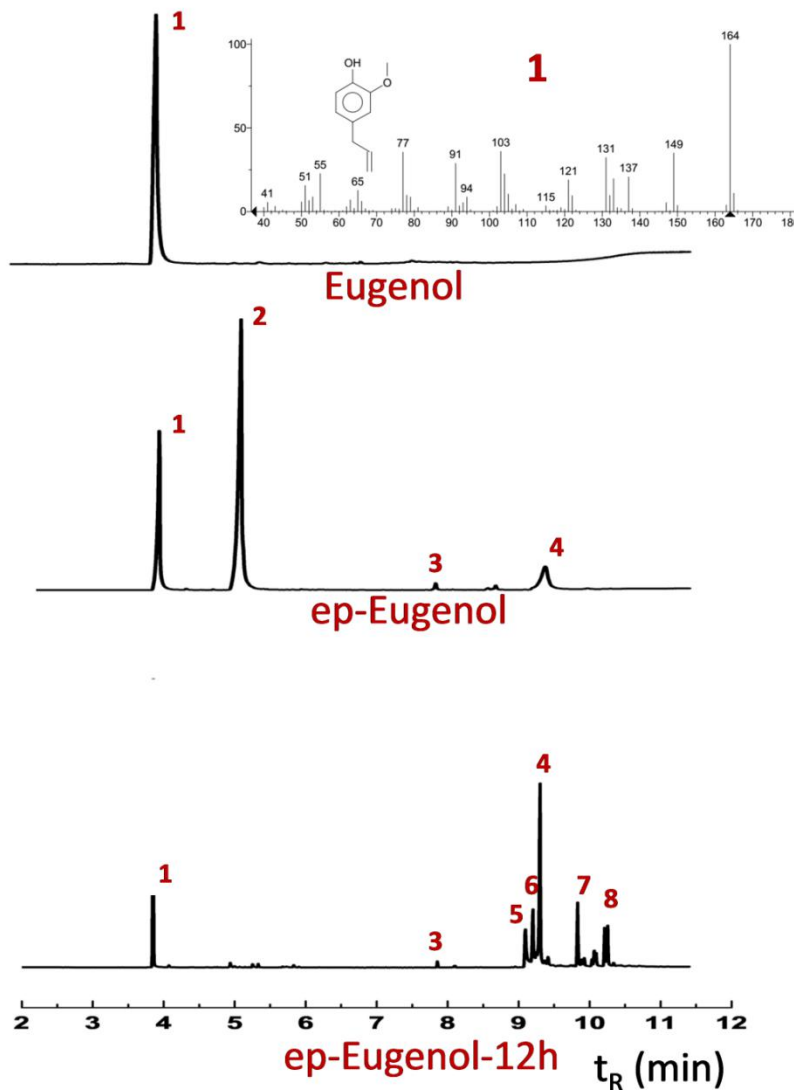
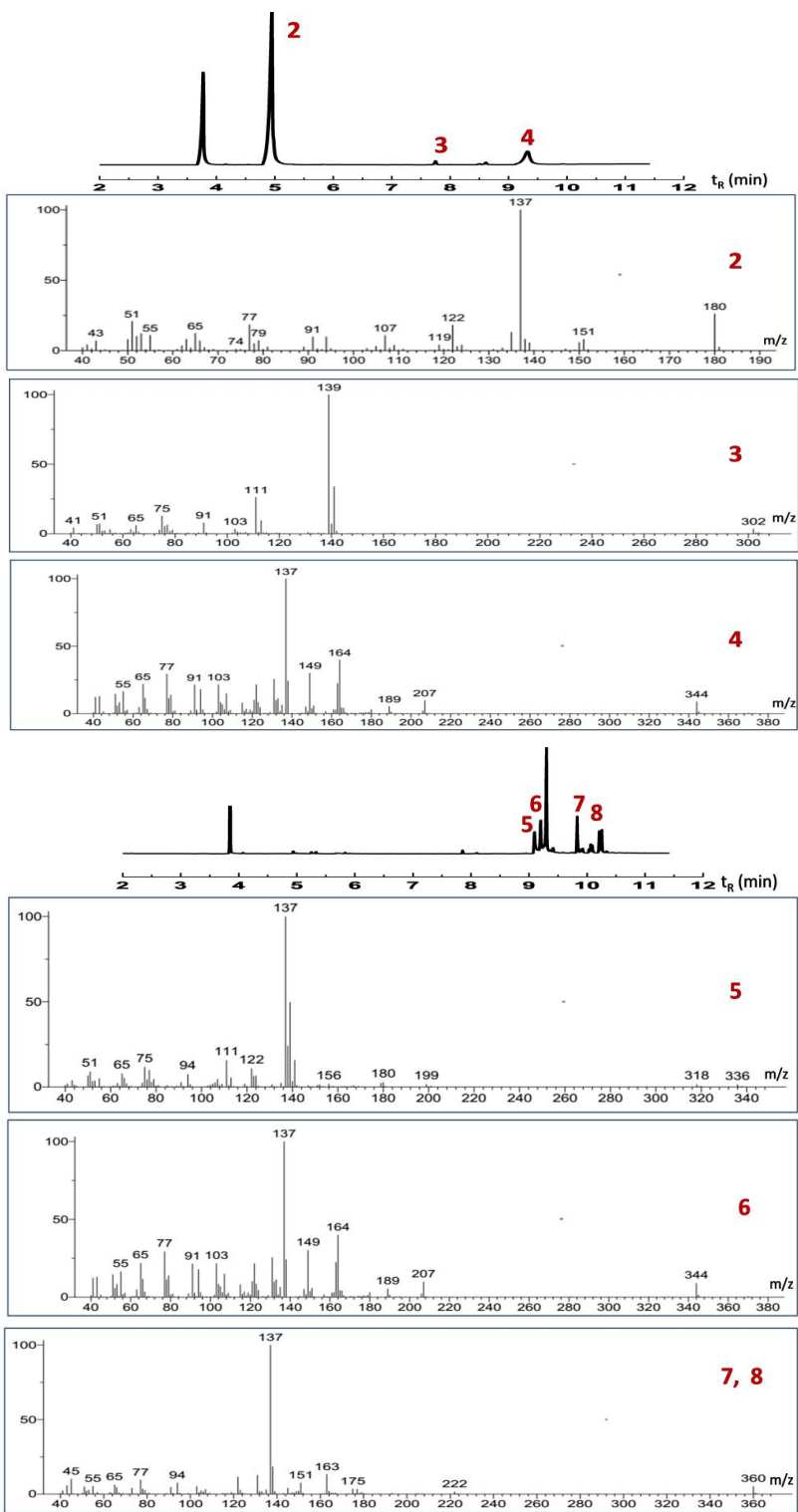


Figure S4. Gas chromatography (GC) traces of Eugenol, ep-Eugenol and ep-Eugenol-12h.

To identify the complex components in the thermochemical conversion process, GC-MS analysis was applied. The peak 1 (retention time 3.8 min) is attributed to the eugenol as the MS spectra shown in the inset. After epoxidation and thermochemical conversion, multiple peaks appeared on the GC traces.

Supporting Information



Supporting Information

Peak 2 shows mass 180 that can be attributed to the epoxidized eugenol. Peak 3 shows a mass of 302 that could correspond to the presence of fragmental structure A (see Figure S5). Peak 4 shows a mass of 344, which indicates that this compound could have subunits C or D in its structure.

Peak 5 shows a mass of 336, indicating the presence of fragmental structure B, and peak 6 could correspond to the subunits C or D because of the mass of 344 observed in its MS spectra. Peaks 7 and 8 show identical MS spectrum, indicating the possibility of identical components in peaks 7 and 8. However, these components did not appear at the same retention time. Therefore, it is speculated that the components associated with peaks 7 and 8 are probably isomers. In addition, based on the mass of 360 shown in the MS spectrum of peaks 7 and 8, the possible structures of these components are shown as E and F (see Figure S5 below).

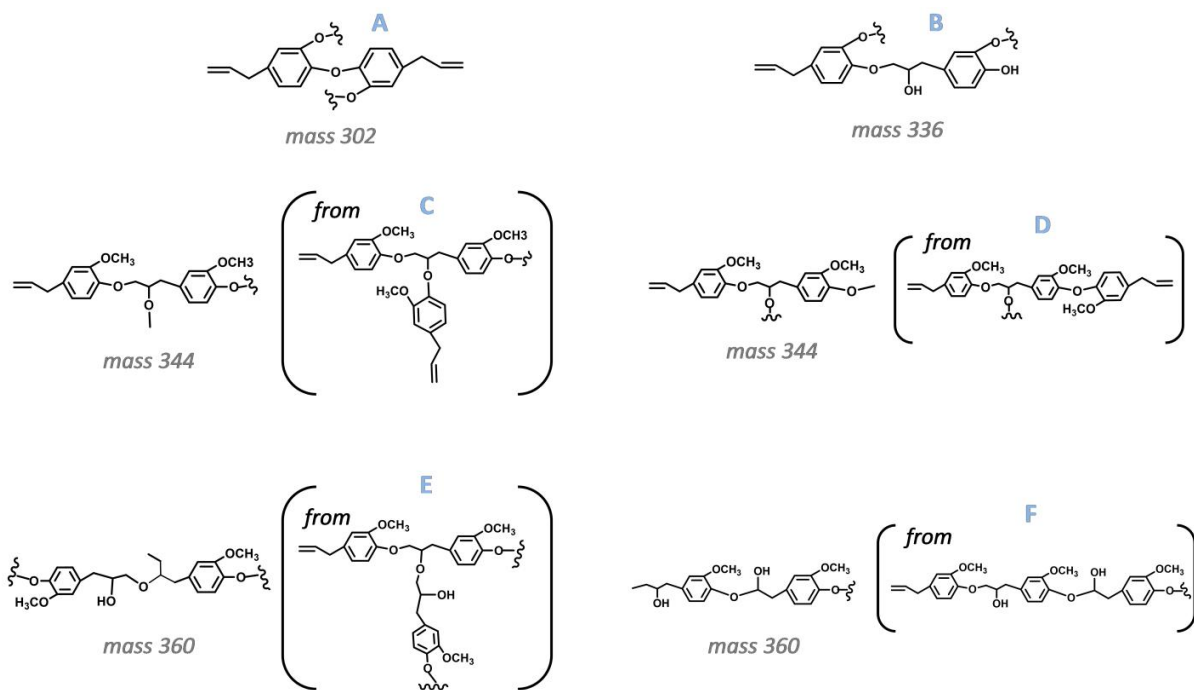


Figure S5. Moieties identified in the eugenol system after epoxidation and thermochemical conversion process.

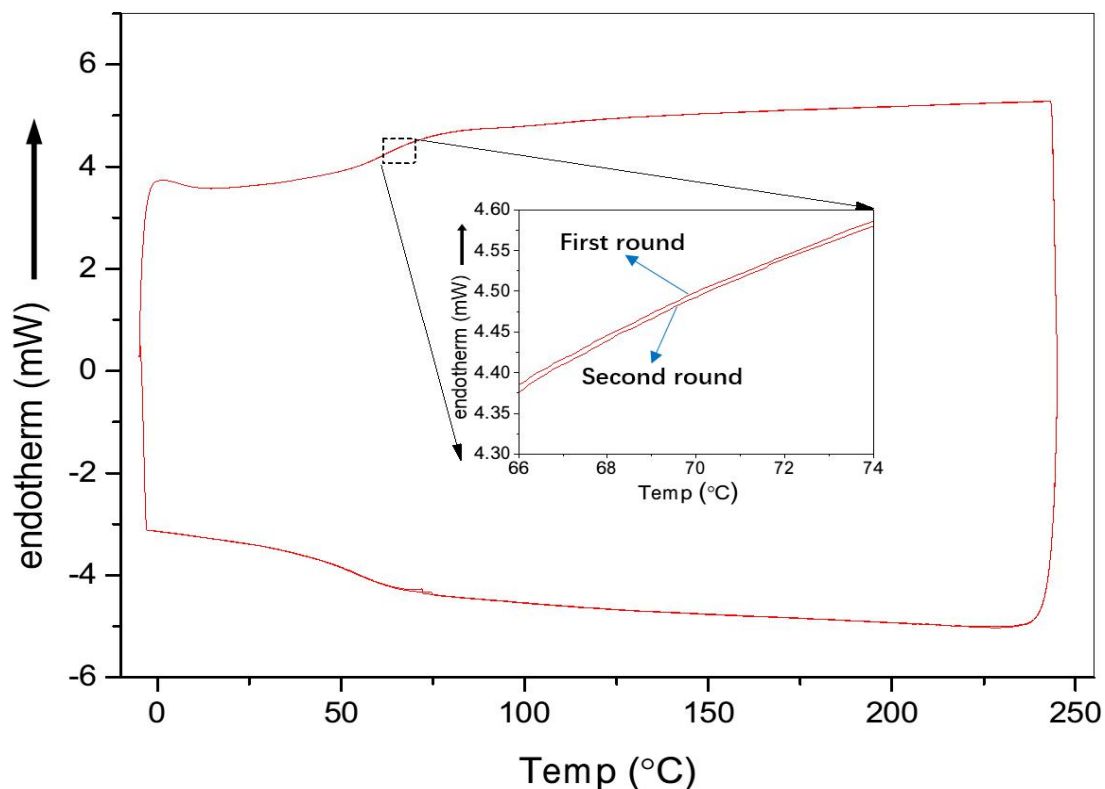


Figure S6. Heating and cooling DSC loop tests for ET-eugenol molecular glass, in which the sample is first heated from 0°C to 240°C at a heating rate of 10 °C/min and then cooled from 240 °C to 0°C at a cooling rate of 10 °C/min as the first round DSC loop test. After the first round DSC loop test, a second round loop test is carried out with the same procedure as the first round. The DSC loop test images show that the endotherm curves relative to the glass transition are almost overlapped between the first and second round tests, indicating a reversible and stable transition between solid and liquid states for ET-eugenol molecular glass.

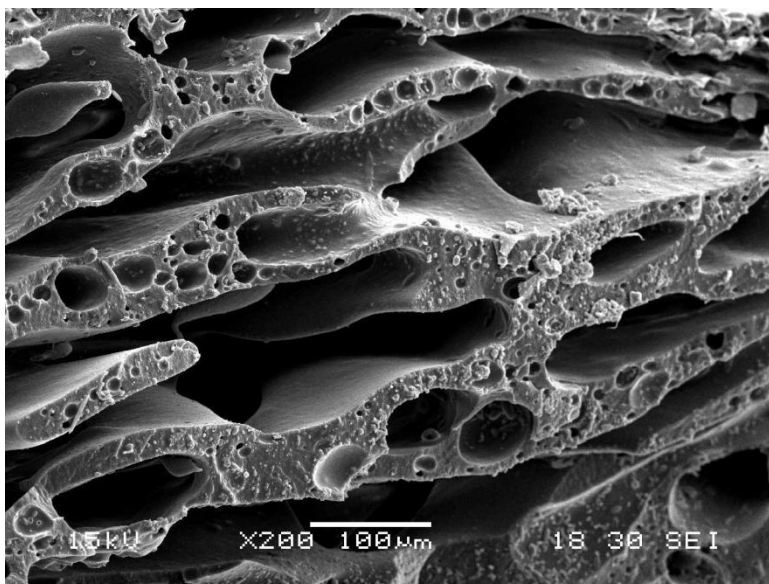


Figure S7. SEM image of the fractured surface of the ET-eugenol/p-ESO (mass ratio of 1:2) blend, where the ET-eugenol components were extracted by butyl acetate.

The morphology of the fractured surface of the blended ET-eugenol/p-ESO (mass ratio of 1:2) etched by butyl acetate is shown above. ET-eugenol components were extracted by butyl acetate and significant phase contrast was identified. The micrograph shows that the ET-eugenol components are dispersed in the p-ESO matrix irregularly. There is a wide size distribution of the ET-eugenol, varying from a few microns to hundred microns. The shapes of the ET-eugenol dispersed in the p-ESO are also diverse, including spherical, ellipsoidal and other irregular shapes.

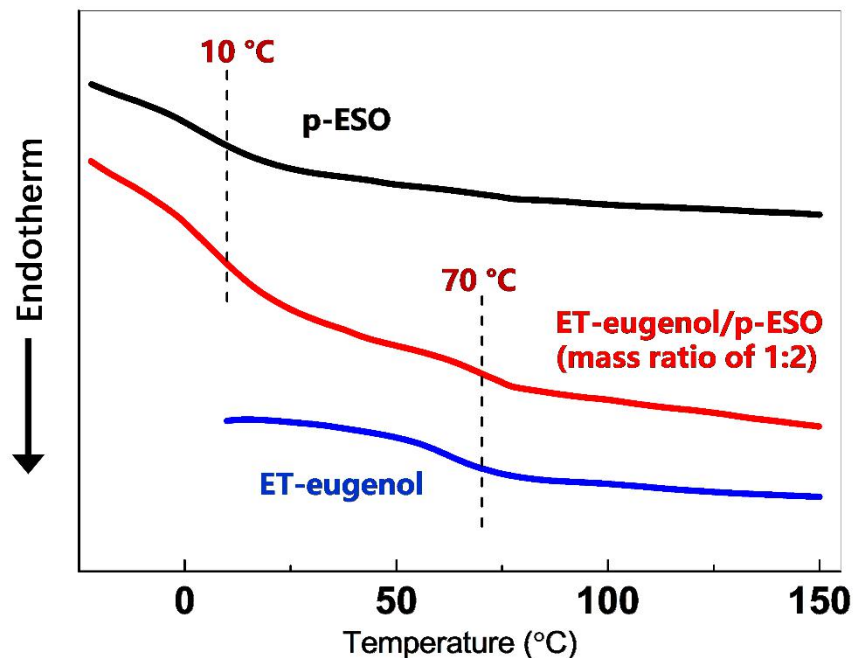


Figure S8. DSC thermograms for p-ESO, ET-eugenol and ET-eugenol/p-ESO (mass ratio of 1:2).

It can be found from Figure S8 that there is an obvious endothermic transition around 10 °C on the p-ESO DSC curve. This transition is associated with the typical glass transition of the p-ESO material. Similarly, the endothermic transition around 70 °C on the ET-eugenol curve is attributed to the glass transition of the ET-eugenol. Compared to the p-ESO and ET-eugenol DSC curves, there are two endothermic transitions on the ET-eugenol/p-ESO (mass ratio of 1:2) DSC curve, indicating two phases (i.e. p-ESO and ET-eugenol) coexist in this system. It can be found that the positions of these two transitions are very closed to the glass transition positions detected on the p-ESO and ET-eugenol DSC curves. This means the p-ESO phase and the ET-eugenol phase are immiscible in the ET-eugenol/p-ESO system, in which the glass transition temperature of one phase is not affected by another phase.

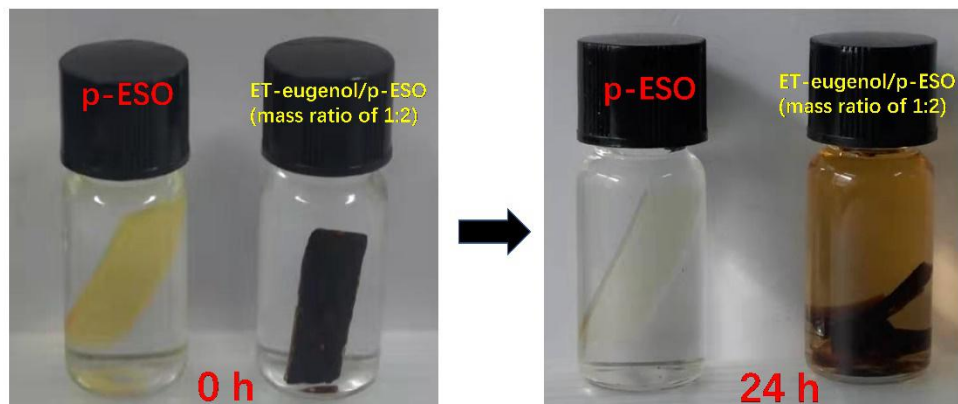


Figure S9. Status comparisons of the p-ESO and the ET-eugenol/p-ESO (mass ratio of 1:2) after being immersed in butyl acetate solvent for 0 h and 24 h.

p-ESO is only swelled and not soluble in butyl acetate solvent as the Figure S9 shown. In contrast, ET-eugenol/p-ESO (mass ratio of 1:2) is partially soluble after being immersed in butyl acetate solvent for 24 h. Table S1 below shows the swelling rate of p-ESO in butyl acetate solvent at room temperature for different times. Table S2 below shows the insoluble content of ET-eugenol/p-ESO (mass ratio of 1:2) after undergoing the extraction of refluxing butyl acetate for different times. It can be found the insoluble content of ET-eugenol/p-ESO (mass ratio of 1:2) is barely changed after undergoing a 72-h extraction. The corresponding value of 77 wt% is much higher than the p-ESO content (66 wt%) in the whole system, indicating partial ET-eugenol still remains in the p-ESO matrix. This is probably due to the insolubility of p-ESO and partial ET-eugenol is still trapped in the matrix incapable of being extracted by solvent.

Table S1

p-ESO	Swelling Rate %			
	12h	24h	36h	48h
	17	23	26	26

Table S2

ET-eugenol/p-ESO (mass ratio of 1:2)	Insoluble Content wt%					
	12h	24h	36h	48h	60h	72h
	93	88	83	80	78	77

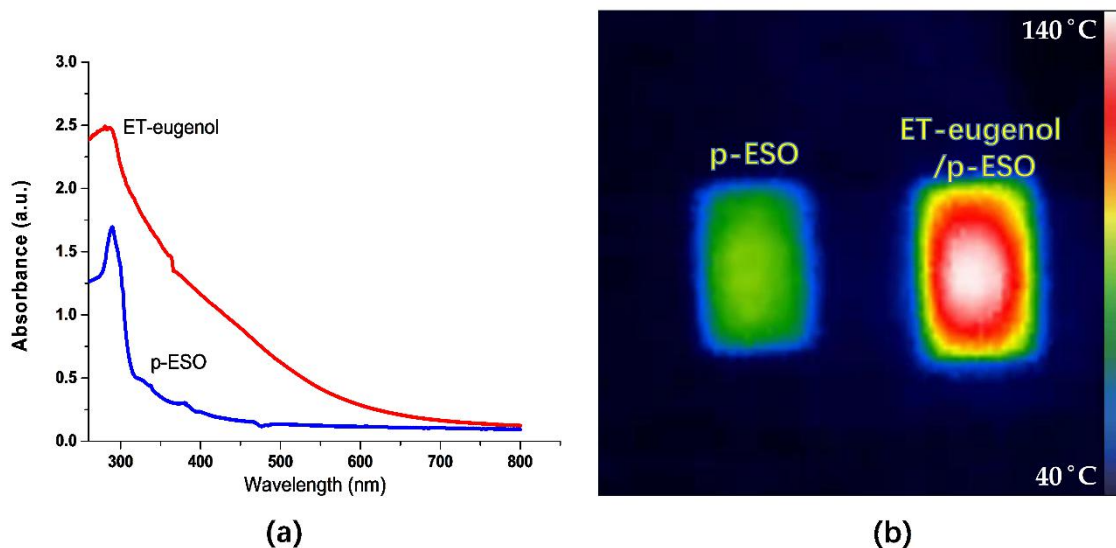


Figure S10. (a) Ultraviolet-visible absorption spectra of ET-eugenol and p-ESO. (b) Infrared image for p-ESO and ET-eugenol/p-ESO (mass ratio of 1:2) after undergoing an ultraviolet light ($\lambda = 320\text{-}390\text{ nm}$, 1800 mw cm^{-2}) radiation for 10 seconds.

The light-to-heat phenomenon is attributed to the electron transition in molecular orbitals with the absorption of light energy, and the resultant energy conversion of light into heat (*Progress in Chemistry*. 2019, *31*(4): 580-596; *Nano Energy*. 2017, *41*: 269-284). For those materials containing conjugated π bonding and π^* antibonding molecular orbitals, the energy gap is generally small. An electron transition from π bonding orbital with low energy level to π^* antibonding orbital with high energy level can occur under the light induction. In the process by which electrons in the excited state fall back to the ground state, partial energy is released as heat and a conversion from light to heat can be realized (*Imaging Science and Photochemistry*. 2017, *35*(4): 464-476).

In terms of the Eugenol-derived molecular glass, the intrinsic phenyl moiety leads to closely spaced energy levels of the electrons via the π bonding and π^* antibonding molecular orbitals, which has good ability to a broad-band light absorption as evidenced by the ultraviolet-visible absorption spectrum shown above (Figure S10a). It can be found that, compared to the p-ESO, ET-eugenol demonstrates a significantly higher capacity of light absorption over the entire wavelength range. Correspondingly, a higher efficient conversion from light to heat can be expected for ET-eugenol. Figure S10b above is the infrared image recorded after p-ESO and ET-eugenol/p-ESO (mass ratio of 1:2) were exposed to an ultraviolet light radiation ($\lambda = 320\text{-}390\text{ nm}$, 1800 mw cm^{-2}) for 10 seconds. ET-eugenol/p-ESO (mass ratio of 1:2) demonstrates an obvious higher temperature distribution compared to p-ESO, indicating a stronger conversion capacity from light to heat.

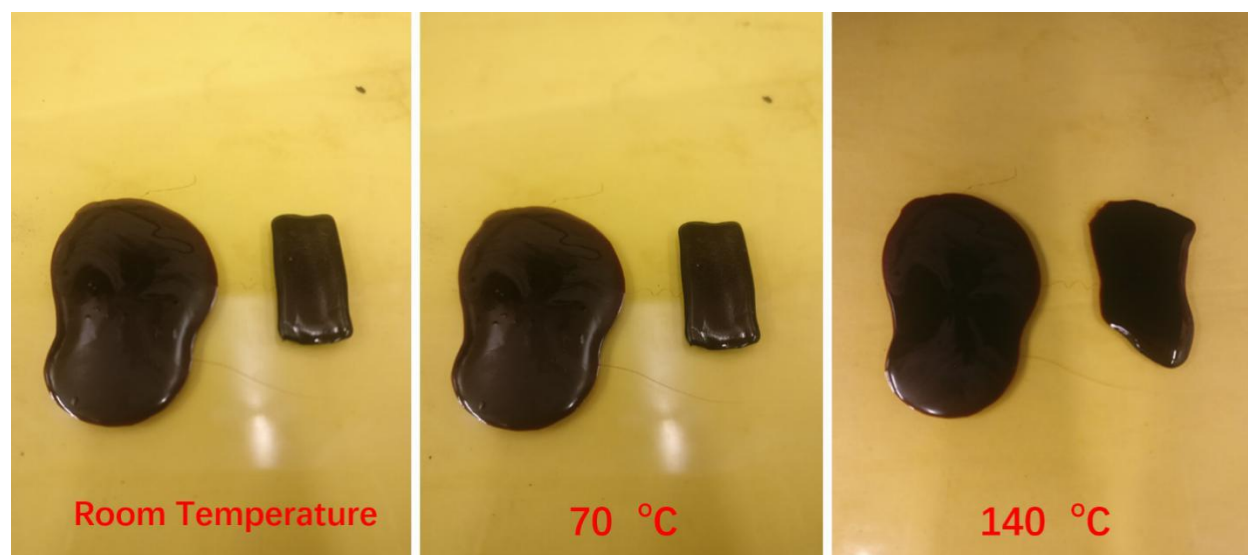


Figure S11. Comparison of shape stabilities of ET-eugenol sample (right) and ET-eugenol/p-ESO (mass ratio of 1:2) sample (left) at different temperatures. Images show that the shape of ET-eugenol/p-ESO sample is kept stable even at temperature of 140 °C, while ET-eugenol has an obvious flow behavior when temperature reaches 140 °C.

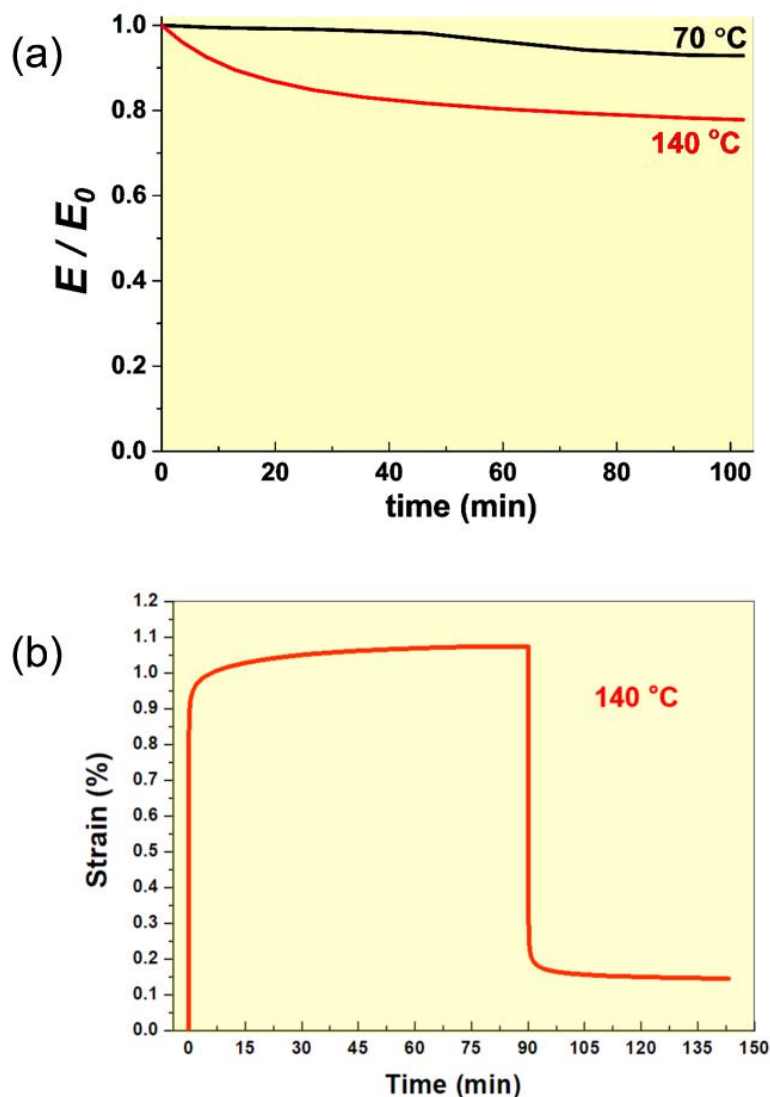


Figure S12. Stress relaxations and creep behavior of ET-eugenol/p-ESO (mass ratio of 1:2) at given temperatures with a strain rate of 1%.

The dimension stability was evaluated via stress relaxations at 70 °C and 140 °C, respectively. As Figure S12 (a) shown, there is a slight modulus decline at 70 °C with time initially, and then the modulus is almost kept constant by a 95% modulus retention. Since the modulus is related to the dimension stability in the stress relaxation test, the final constant modulus means a stable dimension. Compared to the result measured at 70 °C, though the initial modulus decline was

Supporting Information

more obvious at 140 °C, a final 80% modulus retention was still detected, indicating a stable dimension can be obtained even temperature reaches a high value of 140 °C.

The dimension stability was further evaluated via the creep test at 140 °C. As the Figure S12 (b) shown, a rapid deformation recovery was detected after the sample underwent a 1% strain at 140 °C for 90 min, combined with a size retention rate higher than 85%. These results are consistent with the results observed in the stress relaxation and indicate the stable dimension even at high temperature, such as 140 °C.